Published in final edited form as:

J Mol Cell Cardiol. 2017 November ; 112: 74–82. doi:10.1016/j.yjmcc.2017.09.002.

Class I HDACs control a JIP1-dependent pathway for kinesin-microtubule binding in cardiomyocytes

Weston W. Blakeslee[a,b,1], **Ying-Hsi Lin**[a,c,1], **Matthew S. Stratton**[a,c], **Philip D. Tatman**[a,d], **Tianjing Hu**[a,c], **Bradley S. Ferguson**[a,2], and **Timothy A. McKinsey**[a,b,c,*,1]

[a]Department of Medicine, Division of Cardiology, University of Colorado Denver, Anschutz Medical Campus, Aurora, CO, USA

[b]Department of Pharmacology, University of Colorado Denver, Anschutz Medical Campus, Aurora, CO, USA

[c]Consortium for Fibrosis Research & Translation, University of Colorado Denver, Anschutz Medical Campus, Aurora, CO, USA

[d]Medical Scientist Training Program, University of Colorado Denver, Anschutz Medical Campus, Aurora, CO, USA

Abstract

Class I histone deacetylase (HDAC) inhibitors block hypertrophy and fibrosis of the heart by suppressing pathological signaling and gene expression programs in cardiac myocytes and fibroblasts. The impact of HDAC inhibition in unstressed cardiac cells remains poorly understood. Here, we demonstrate that treatment of cultured cardiomyocytes with small molecule HDAC inhibitors leads to dramatic induction of c-Jun amino-terminal kinase (JNK)-interacting protein-1 (JIP1) mRNA and protein expression. In contrast to prior findings, elevated levels of endogenous JIP1 in cardiomyocytes failed to significantly alter JNK signaling or cardiomyocyte hypertrophy. Instead, HDAC inhibitor-mediated induction of JIP1 was required to stimulate expression of the kinesin heavy chain family member, KIF5A. We provide evidence for an HDAC-dependent regulatory circuit that promotes formation of JIP1:KIF5A:microtubule complexes that regulate intracellular transport of cargo such as autophagosomes. These findings define a novel role for class I HDACs in the control of the JIP1/kinesin axis in cardiomyocytes, and suggest that HDAC inhibitors could be used to alter microtubule transport in the heart.

Keywords

Histone deacetylase (HDAC); Cardiomyocyte; Microtubule; Kinesin heavy chain isoform 5A (KIF5A); C-Jun amino-terminal kinase (JNK); JNK-interacting protein (JIP)

*Corresponding author at: Department of Medicine, Division of Cardiology, University of Colorado Denver, Anschutz Medical Campus, Aurora, CO, USA. timothy.mckinsey@ucdenver.edu (T.A. McKinsey).

[1]Equal contributors.

[2]Present address: Department Agriculture, Nutrition, & Veterinary Sciences, University of Nevada, Reno, NV, USA.

1. Introduction

Histone deacetylases (HDACs) catalyze removal of acetyl groups from lysine residues in numerous proteins. HDACs have mainly been studied in the context of chromatin, where they deacetylate nucleosomal histone tails and alter the electrostatic properties of chromatin in a manner that represses or promotes gene expression. However, HDACs have non-histone substrates, and proteomic studies have revealed that thousands of proteins undergo reversible lysine acetylation [1–3].

The 18 mammalian HDACs are clustered into four classes: class I HDACs (1, 2, 3 and 8), class II HDACs (4, 5, 6, 7, 9 and 10), class III HDACs (SirT 1–7) and class IV (HDAC11) [4]. Class II HDACs are further separated into two subclasses, IIa (HDACs 4, 5, 7 and 9) and IIb (HDACs 6 and 10). Class I, II and IV HDACs are zinc-dependent enzymes, while class III HDACs, which are also known as sirtuins, require NAD^+ as a co-factor for catalytic activity.

In response to pathological stresses such as myocardial infarction and chronic hypertension, the heart undergoes a remodeling process that is typified by cardiomyocyte hypertrophy and interstitial fibrosis [5]. Pathological cardiac remodeling can result in impaired systolic and diastolic ventricular function, and ultimately heart failure. Heart failure currently afflicts approximately 6 million adults in the United States alone, and this number is projected to rise to 8 million by 2030 [6]. Given that the 5-year mortality rate following first admission for heart failure is over 40%, there is a crucial need to develop novel therapeutic strategies for this devastating condition.

Small molecule inhibitors of HDACs have shown promise in a variety of pre-clinical models of heart failure [7]. For example, trichostatin A (TSA) is able to reverse pre-existing cardiac hypertrophy and left ventricular (LV) dysfunction in a mouse pressure overload model [8]. TSA is a ‘pan’ inhibitor that targets all zinc-dependent HDACs [9], and it has long been postulated that the anti-hypertrophic action of pan-HDAC inhibitors is due to blockade of class I HDAC activity [10]. Consistent with this notion, experiments with cultured cardiomyocytes have implicated class I HDACs in the control of cardiac hypertrophy [11]. In vivo, a derivative of apicidin, which is a fungal metabolite that selectively inhibits class I HDACs, partially blocked cardiac hypertrophy in a mouse pressure overload model [12]. More recently, apicidin itself was found to reduce hypertrophic gene expression in response to pressure overload in mice [13]. Furthermore, selective class I HDAC inhibition with Mocetinostat (MGCD0103) blocked cardiac fibrosis in response to chronic angiotension II infusion [14], and blunted progression of cardiac fibrosis in a chronic rat MI model, resulting in improved function of the heart [15].

Class I HDACs, particularly HDACs -1, -2 and -3, are canonical epigenetic regulatory proteins. These HDACs are present in the nucleus in large multi-protein complexes referred to as Sin3, NuRD, CoREST and NCoR/SMRT, which are recruited to gene regulatory elements by sequence-specific DNA binding transcription factors [16,17]. Consistent with this function, suppression of cardiac hypertrophy and fibrosis by class I HDAC inhibitors have been linked to changes in gene expression. For example, HDAC inhibitor treatment of

cardiomyocytes leads to increased expression of the anti-hypertrophic transcription factor, krüppel-like factor 4 (KLF4) [18] and increased expression of an anti-hypertrophic microRNA (miR-9) [19], with subsequent blunting of cardiomyocyte growth. In cardiac fibroblasts, HDAC inhibitors trigger cyclin-dependent kinase inhibitor gene expression, which limits expansion of fibrogenic myofibroblasts [14,20], and they stimulate expression of miR-133, which suppresses pro-fibrotic gene expression [21].

Emerging data also demonstrate a role for class I HDACs in the control of cardiac kinase signaling networks. Class I HDAC inhibition in the heart was shown to promote expression of tuberous sclerosis complex 2 (TSC2), which is an inhibitor of pro-hypertrophic mechanistic target of rapamycin (mTOR) kinase signaling [13]. Furthermore, we have found that class I HDAC inhibition blocks cardiomyocyte hypertrophy by suppressing extracellular signal-regulated kinase (ERK) through upregulation of a mitogen-activated protein kinase (MAP kinase) phosphatase, DUSP5, which dephosphorylates ERK1/2 [22].

The present study was designed to further address the potential of class I HDACs to influence cardiomyocyte MAP kinase signaling. We demonstrate that class I HDAC inhibition stimulates dramatic expression of the c-Jun amino-terminal kinase (JNK)-interacting protein-1 (JIP1) scaffolding protein in cardiomyocytes. Surprisingly, JIP1 does not markedly affect JNK signaling in the cells. Instead, JIP1 regulates expression of kinesin heavy chain isoform 5A (KIF5A), and promotes association of KIF5A with microtubules. These findings suggest a previously unrecognized role for class I HDACs in the control of microtubule dynamics in cardiomyocytes.

2. Materials and methods

2.1. Reagents

Trichostatin A (TSA) was obtained from Sigma and used at a final concentration of 200 nM. MGCD0103 was purchased from Selleck Chemicals and used at 1 μM final concentration. Phenylephrine (PE) and actinomycin D were purchased from Sigma and used at final concentrations of 10 μM and 1 μg/mL, respectively.

2.2. Neonatal rat ventricular myocytes

Neonatal rat ventricular myocytes (NRVMs) were prepared from hearts of 1- to 3-day old Sprague Dawley rats, as previously described (22). Cells were cultured overnight on plates coated with gelatin (0.2%; Sigma) in Dulbecco's Modified Eagle's Medium (DMEM) containing calf serum (10%), L-glutamine (2 mM), and penicillin–streptomycin. After overnight culture, cells were washed with serum-free medium and maintained in DMEM supplemented with L-glutamine, penicillin–-streptomycin, and Neutridoma-SP (0.1%; Roche Applied Science), which contains albumin, insulin, transferrin, and other defined organic and inorganic compounds. For the starvation experiments shown in Fig. 7, NRVMs were maintained in Neutridoma-containing DMEM for 24 h followed by Neutridoma-free medium for 24 additional hours. Finally, cells were shifted to Neutridoma-free DMEM without glucose for 8 h prior to preparing protein homogenates for immunoblotting.

2.3. Adenovirus production

Recombinant adenoviruses encoding shRNAs to target rat JIP1 were prepared using the BLOCK-it™ Adenoviral Expression System (Invitrogen). Oligonucleotide targeting sequences are shown in Table 1. Top and bottom strands were annealed and ligated into the pENTR/U6 vector (Invitrogen). Positive subclones were recombined with the pAd/BLOCK-it™-DEST vector (Invitrogen) and then transfected into 293A cells using Fugene 6 (Roche). PCR was employed to construct full-length JIP1 (JIP1-FL, amino acids 1–707) and N-terminally truncated JIP1 (JIP1-ΔN, amino acids 94–707) expression vectors using mouse JIP1 as a template (Addgene plasmid #51699) [23]. JIP1-FL was cloned into pcDNA3.1 with an in-frame N-terminal FLAG epitope tag. JIP1-ΔN was cloned into pcDNA3.1 with an in-frame N-terminal Myc epitope tag. Next, both cDNAs were excised and subcloned into pENTR2b. LR-recombination was then performed to transfer the JIP1 cDNAs from pENTR2b to pAd-CMV-V5 DEST. Recombined viral vectors were transfected into 293A cells using polyethyleneimine (PEI). Viruses were amplified and recovered from 293A cells, and titered using the Sea-Plaque agarose method. All viruses were used at a multiplicity of infection (MOI) of 50 at the time of plating.

2.4. Immunoblotting

Cells were lysed in radioimmunoprecipitation assay buffer (RIPA) containing 50 mM Tris (pH 8.0), 150 mM NaCl, 0.1% SDS, 0.5% sodium deoxycholate, 1% NP-40 and HALT™ protease/phosphatase inhibitor mixture (Thermo Fisher). Cellular lysates were sonicated before clarification by centrifugation. Proteins were resolved by SDS-PAGE, transferred to nitrocellulose membranes (BioRad) and probed with antibodies for JIP1 (Santa Cruz Biotechnology, sc-25267), total JNK (Santa Cruz Biotechnology, sc-474), phospho-JNK (Cell Signaling Technology, 4668), cFos (Cell Signaling Technology, 4384), acetylhistone H3 (Cell Signaling Technology, 4499), KIF5A (Abcam, ab5268), calnexin (Santa Cruz Biotechnology, sc-11397), Myc (Santa Cruz Biotechnology, sc-40), and GAPDH (Invitrogen, AM4300). Immunoblotting with an anti-LC3 antibody (Sigma, L7543) was performed using PVDF membrane (BioRad).

2.5. Indirect immunofluorescence

NRVMs were fixed with 4% paraformaldehyde at room temperature for 10 min. Cells were permeabilized with PBS containing 0.2% Triton X-100 for 15 min, and blocked with PBS containing 10% FBS for 30 min at room temperature. Then, cells were incubated in primary antibodies (Myc, Santa Cruz Biotechnology, sc-40, 1:200; FLAG, Sigma, F1804, 1:200; α-actinin, Sigma, A7811L, 1:1000) for 1 h. Secondary antibodies (Anti Mouse Alexa Fluor® 488, A11029, 1:1000; Anti Rabbit Alexa Fluor® 488, A11034, 1:1000) were applied for 30 min at room temperature. Coverslips were mounted on glass slides using mounting medium (Vector Laboratories, H-1200). Confocal images were obtained via an Olympus FLUOVIEW FV1000 confocal laser scanning microscope (UC Denver, Advanced Light Microscopy Core). For data shown in Fig. 6, NRVMs were grown on gelatin-coated 6-well plates and stained with primary antibodies for α-tubulin (Santa Cruz, sc-23948, 1:1000), acetyl-tubulin (Santa Cruz, sc-23950, 1:200) and α-actinin (Sigma, A7811, 1:200), and secondary antibodies (Anti Mouse Alexa Fluor® 488, A11029, 1:1000; Anti Mouse Alexa

Fluor® 555, A21422, 1:1000). Images were captured using EVOS FL Cell Imaging System (Life Technologies, AMF4300). NRVM cell area was quantified based on α-actinin staining using Image J software.

2.6. Quantitative PCR analysis

For assessment of JIP1, KIF5A, KIF5B and KIF5C mRNA expression, RNA was harvested from NRVMs using Trizol, as previously described (Spiltoir et al., 2013). cDNA was prepared with the VERSO cDNA Synthesis Kit (Life Technologies) and qPCR was accomplished with DyNAmo Flash SYBR Green qPCR kit (Life Technologies) using a StepOnePlus Real-Time PCR System (Life Technologies). Relative expression was calculated using the $2^{-\Delta\Delta CT}$ method with normalization to 18S RNA expression. qPCR primer sequences are shown in Table 1.

2.7. RNA-sequencing analysis

RNA was harvested from NRVMs using the Roche High Pure RNA Isolation Kit, and cDNA sequencing libraries were prepared using the Ovation RNA Seq System V 1–16 for Model Organisms (Rat) (NUGEN). Libraries were sequenced by the University of Colorado Denver Genomics and Microarray Core on a HiSeq 2500 (Illumina). All analysis was performed using Rat RN5 genome and RN5 RefSeq gene annotations. Raw and processed RNA-seq data were deposited to the GEO online database (http://www.ncbi.nlm.nih.gov/geo/) under accession numbers GEO: (GSE102609). All RNA-seq datasets were aligned to the transcriptome using Tophat2 (version 2.0.11) (http://www.genomebiology.com/2013/14/4/R36/abstract). Gene expression values were quantified using Cufflinks and Cuffnorm (version 2.2.0) [24].

2.8. Microtubule binding assay

The procedure was performed according to the manufacturer's instructions (Cytoskeleton, CO, US), with slight modifications. Briefly, NRVMs plated on 10-cm plates (1.8×10^6/plate) were infected with Ad-shControl or Ad-shJIP1 at the time of plating for 24 h prior to treatment with TSA or vehicle control for 48 additional hours. NRVMs were lysed in HEM buffer (80 mM HEPES pH 6.8, 5 mM $MgCl_2$, 2 mM EGTA, 0.15% (v/v) Triton X-100 containing HALT™ protease/phosphatase inhibitor mixture (Thermo Fisher)) and protein lysates (250 μg) were mixed with taxol-stabilized microtubules (0.4 nM). Reactions were incubated at room temperature for 30 min and subsequently loaded onto taxol-supplemented cushion buffer and centrifuged at 100,000 × *g* for 40 min at room temperature. Soluble fraction and pellets (microtubule fractions) were equilibrated in Laemmli buffer, resolved by SDS-PAGE, and analyzed by immunoblotting.

3. Results

3.1. HDAC inhibition stimulates JIP1 expression in cardiomyocytes

We previously demonstrated that class I HDAC inhibition potently suppresses phosphorylation of JNK in cardiomyocytes [22]. JIP1 is a scaffold protein that can positively or negatively regulate JNK signaling depending on its abundance [25]. To begin to address whether JIP1 plays a role in HDAC inhibitor-mediated suppression of JNK phosphorylation,

cultured neonatal rat ventricular myocytes (NRVMs) were treated for 48 h with TSA, and JIP1 protein levels were assessed by immunoblotting. Expression of two isoforms of JIP1 was dramatically increased in TSA-treated NRVMs, but not in cells exposed to vehicle control or the hypertrophic agonist phenylephrine (PE) (Fig. 1A). The two JIP1 isoforms, referred to as JIP1 long (L) and JIP1 short (S), were also stimulated by the class I HDAC inhibitor, MGCD0103, in either the absence or presence of PE (Fig. 1B). Elevated JIP1 levels correlated with reduced basal and PE-stimulated JNK phosphorylation (Fig. 1A and B).

The transcription inhibitor, actinomycin D, was employed to test whether HDAC inhibitors enhance JIP1 expression via a transcriptional or post-transcriptional mechanism (Fig. 1C). Pre-treatment of NRVMs with actinomycin D for 30 min blocked the ability of TSA to induce JIP1 protein expression (Fig. 1D). Consistent with this, both TSA and MGCD0103 stimulated JIP1 mRNA expression in NRVMs, as determined by qPCR analysis (Fig. 1E).

Next, an experiment was conducted to compare the kinetics of TSA-mediated JIP1 induction to the ability of the HDAC inhibitor to block agonist-dependent JNK phosphorylation. NRVMs were pre-treated with TSA for 2, 4, 8, 24 or 48 h prior to stimulation with PE for 2 h. Strikingly, as JIP1 levels rose in TSA-treated NRVMs, there was concomitant suppression of agonist-induced JNK phosphorylation (Fig. 1F). The correlation was most pronounced with JIP1 (L), which was prominently induced 24 h post-TSA treatment, when phospho-JNK levels reached a nadir.

3.2. JIP1 does not govern HDAC inhibitor-mediated suppression of JNK

Gain- and loss-of-function experiments were performed to directly address whether JIP1 controls JNK phosphorylation in cardiomyocytes. Adenoviruses were constructed to overexpress full-length JIP1 (JIP1-FL) and an N-terminally truncated version of JIP1 (JIP1-ΔN) (Fig. 2A). Rationale for creating the truncation mutant was based on a prior description of a form of JIP1 produced via an internal start methionine residue, methionine-101 [26]. Upon infection of NRVMs with the viruses, both proteins were efficiently expressed and localized to the cytoplasmic compartment (Fig. 2B). Ectopic expression of either JIP1-FL singly or in combination with JIP1-ΔN blunted PE-induced JNK phosphorylation, while JIP1-ΔN alone failed to impact JNK phosphorylation in NRVMs (Fig. 2C). Note that we refer to these proteins as JIP1-ΔN and JIP1-FL because we have not confirmed that they are identical to JIP1 (S) and JIP1 (L), respectively.

Subsequently, adenovirus encoding shRNA targeting JIP1 mRNA transcripts (Ad-shJIP1) was employed to knockdown endogenous JIP1 expression. Ad-shJIP1 infection of NRVMs led to dramatic reduction in basal and TSA-induced JIP1 expression compared to cells infected with Ad-shControl (Fig. 2D, top panel). Although JIP1 knockdown appeared to modestly blunt PE-mediated JNK phosphorylation, it failed to rescue JNK phosphorylation in the presence of TSA (Fig. 2D, middle panel). Thus, although ectopic JIP1-FL was sufficient to suppress JNK phosphorylation (Fig. 2C), the mechanism by which HDAC inhibitors block JNK phosphorylation does not appear to involve upregulation of endogenous JIP1, since TSA still inhibited JNK in NRVMs where JIP1 expression was nearly undetectable.

3.3. JIP1 controls HDAC inhibitor-mediated gene expression in cardiomyocytes

Whole transcriptome RNA-seq analysis was performed to further explore the functional consequences of JIP1 induction by HDAC inhibitors in cardiomyocytes. NRVMs were infected with Ad-shControl or Ad-shJIP1 for 24 h prior to treatment with TSA or vehicle control for 48 additional hours. TSA significantly altered expression of 1762 mRNA transcripts in a positive or negative manner, as illustrated by the heat map (Fig. 3A). For 362 TSA-regulated genes, JIP1 knockdown significantly reversed expression by at least 10%. Gene set enrichment analysis (GSEA) of this subset revealed that JIP1 controls expression of genes associated with cytoskeletal dynamics and vesicle trafficking (Fig. 3B). We then focused on TSA-regulated genes that were completely returned to baseline by JIP1 knockdown. Network interaction analysis of this subset indicated the magnitude and direction of the expression changes between JIP1 knockdown NRVMs treated with TSA and control cells treated with TSA (Fig. 3C). Expression of the gene encoding the KIF5A motor protein was the most dramatically induced by TSA, and brought to baseline levels in NRVMs in which JIP1 was knocked down.

3.4. HDAC inhibition stimulates cardiomyocyte KIF5A expression in a JIP1-dependent manner

Quantitative PCR analysis of RNA from independent samples confirmed that TSA stimulates KIF5A mRNA expression in NRVMs through a mechanism that is dependent on JIP1 (Fig. 4A). TSA did not stimulate expression of the related kinesin heavy chain family member, KIF5B, although a modest induction of the transcript was noted in JIP1 knockdown cells (Fig. 4B). In contrast, TSA robustly increased expression of a third family member, KIF5C, but this occurred in a JIP1-independent manner (Fig. 4C). These findings suggest that JIP1 predominantly regulates KIF5A expression in cardiomyocytes. Interestingly, ectopic expression of JIP1-ΔN or JIP1-FL, in the absence of an HDAC inhibitor, failed to induce KIF5A mRNA expression, demonstrating that JIP1 is necessary but not sufficient to stimulate the gene encoding this kinesin family member (Fig. 4D).

Increased expression of JIP1 protein in NRVMs treated with TSA correlated with enhanced production of KIF5A protein levels (Fig. 4E). Adenoviruses encoding shRNAs that target distinct regions of the JIP1 mRNA transcript equivalently reduced TSA-mediated stimulation of KIF5A protein expression, suggesting an on-target mechanism-of-action. Furthermore, JIP1 knockdown effectively blunted KIF5A protein expression in NRVMs treated with the class I HDAC inhibitor, MGCD0103 (Fig. 4E), illustrating a role for HDAC1, -2 and/or -3 in the control of this kinesin family member.

3.5. HDAC inhibition in cardiomyocytes increases the capacity of KIF5A and JIP1 to bind to microtubules

JIP1 has been shown to regulate organelle transport along microtubules by binding to kinesin heavy chain proteins [27]. As such, an experiment was performed to address the possibility that HDAC inhibition in cardiomyocytes increases microtubule binding activity of KIF5A and JIP1 (Fig. 5A). NRVMs were infected with Ad-shControl or Ad-shJIP1 and treated with TSA or vehicle control for 24 h. Protein homogenates were then incorporated into an in vitro binding assay with polymerized microtubules. TSA treatment led to robust

binding of JIP1 and KIF5A to polymerized microtubules (Fig. 5B). In contrast, in NRVMs in which JIP1 expression was knocked down with Ad-shJIP1, KIF5A microtubule binding was nearly abolished. Similar results were obtained employing homogenates from NRVMs treated with the class I HDAC inhibitor, MGCD0103 (Fig. 5C).

3.6. JIP1 knockdown alters microtubule morphology but does not block cardiomyocyte hypertrophy

Next, experiments were performed to further explore the relationship between JIP1 and microtubules in cardiomyocytes. Indirect immunofluorescence failed to reveal overt difference in microtubule morphology in unstimulated or PE-treated NRVMs in which JIP1 expression was reduced by Ad-shJIP1 compared to control cells (Fig. 6A). However, knockdown of JIP1 did appear to shift acetyl-α-tubulin from a predominantly perinuclear localization to a more diffuse distribution within NRVMs, and this was particularly evident upon stimulation with PE (Fig. 6B, lower right-hand corner). However, despite this difference, JIP1 knockdown had no impact on PE-mediated hypertrophic growth of NRVMs, and did not reduce agonist-dependent expression of the prohypertorphic marker gene, *Nppa* (Fig. 6C–E).

3.7. JIP1 alters autophagy in cardiomyocytes

JIP1 regulates axonal transport of autophagosomes in neurons [28,29]. To begin to address whether JIP1 regulates autophagy in cardiomyocytes, we monitored levels of the autophagosome adaptor protein LC3 in NRVMs. JIP1 knockdown led to a pronounced reduction in basal levels of LC3-II, which is the autophagosome membrane-bound form of the protein (Fig. 7A and B). Starvation led to an increase in LC3-II abundance in both control and JIP1 knockdown NRVMs. However, since the pre-starvation amount of LC3-II was reduced by JIP1 knockdown, the magnitude of starvation-induced LC3-II accumulation in these cells was less than in controls. These findings suggest a regulatory role for JIP1 in the control of cardiomyocyte autophagy.

4. Discussion

HDACs and HDAC inhibitors have long been known to regulate cardiomyocyte hypertrophy and expression of pro- and anti-hypertrophic genes in the heart. However, little is known about the impact of HDAC inhibition on the regulation of cardiac genes that control processes other than cell growth. Here, we describe a novel role for HDACs, class I HDACs in particular, in the control of a regulatory circuit that is known to govern intracellular transport of cargo such as mitochondria and autophagosomes. HDAC inhibition leads to induction of the gene encoding JIP1. JIP1 in turn promotes expression of the KIF5A motor protein and enhances the ability of KIF5A to engage polymerized microtubules (Fig. 7C), thus setting the stage for dynamic alterations in organelle movement along microtubules in cardiomyocytes.

We initiated the current studies because of our prior demonstration that HDAC inhibition potently suppresses phosphorylation of JNK in cardiomyocytes [22]. We hypothesized that HDAC inhibition blocks JNK phosphorylation by altering expression of JIP1, since JNK

signaling is sensitive to JIP1 levels [25]. Indeed, the kinetics of JIP1 induction upon HDAC inhibition correlated well with blockade of JNK phosphorylation (Fig. 1F). However, while overexpression of ectopic JIP1 reduced JNK phosphorylation (Fig. 2C), JIP1 knockdown failed to rescue JNK phosphorylation in HDAC inhibitor-treated NRVMs (Fig. 2D). Thus, the mechanism by which HDAC inhibition blocks JNK phosphorylation in NRVMs does not involve JIP1 and remains unknown.

The function of JIP1 in striated muscle is poorly understood. Work published over 15 years ago showed that transient transfection of a JIP1 expression plasmid into NRVMs reduced expression of luciferase reporter genes under the control of promoters from genes (e.g. *Nppa*) that are activated during hypertrophy [30]. In a model of simulated myocardial infarction induced by metabolic inhibitors, adenovirus-mediated overexpression of JIP1 was shown to blunt apoptosis of cultured adult rabbit cardiomyocytes in a manner that correlated with reduced JNK phosphorylation [31]. In skeletal muscle, adenoviral-mediated overexpression of JIP1 prevented degeneration of tibialis anterior muscles in the mdx:Myo−/− mouse model of muscular dystrophy [32]. We did not observe a difference in PE-mediated induction of endogenous *Nppa* expression in JIP1 knockdown cells versus control NRVMs, and reducing JIP1 expression did not overtly alter agonist-dependent hypertrophic growth of cardiomyocytes or cell viability (Fig. 6). Thus, the possible involvement of JIP1 in cardiomyocyte hypertrophy and/or death awaits further investigation.

JIP1 function is better understood in the brain. In neurons, JIP1 binds kinesin heavy chain motor proteins to promote transport of cargo along microtubules. JIP1/kinesin-regulated cargo includes amyloid beta precursor protein-positive vesicles, synaptic vesicles and mitochondria [27,33–35]. Furthermore, JIP1 regulates axonal transport of autophagosomes [28,29]. It is interesting to note that autophagy in the heart is highly sensitive to HDAC inhibition [8,36], suggesting a possible role for JIP1 in the control of cardiac autophagic flux. Consistent with this, we found that JIP1 knockdown in NRVMs diminished the level of LC3-II, which is involved in the formation of autophagosomes (Fig. 7). These findings suggest that JIP1 plays a previously unrecognized role in the control of autophagy in the heart.

The mechanism by which HDAC inhibitors stimulate JIP1 expression may involve the transcriptional repressor RE-1 silencing transcription factor (REST). In transfected pancreatic β cells, REST potently suppressed expression of islet-brain 1 (IB1), which is the rat and human homologue of JIP-1, by direct binding to the IB1 promoter [37]. REST is known to repress gene expression through recruitment of HDACs to regulatory elements and, consistent with this, TSA was able to derepress the IB1 promoter in a variety of cell types [37,38]. Thus, it is possible that REST:class I HDAC complexes suppress JIP1 expression in NRVMs.

JIP1 can regulate JNK function through a variety of mechanisms, which include functioning as a scaffold for MAP2Ks, MAP3Ks and dual specificity phosphatases [39]. The mechanism by which HDAC inhibitors stimulate KIF5A expression via JIP is unlikely to involve JNK, since JNK phosphorylation is nearly abolished in HDAC inhibitor-treated cells (Fig. 1). The cytoplasmic localization of JIP1 (Fig. 2B), coupled with the presence of SH3 and PTB

protein-protein interaction modules within JIP1, leads us to posit that the scaffold potentiates JNK-independent signaling events that activate downstream transcriptional effectors of the *Kif5a* gene.

Whether class I HDAC-mediated control of KIF5 via JIP1 occurs in non-cardiac cells is unknown. Given the link between KIF5A mutations and disorders such as hereditary spastic paraplegia [40], as well as the recent demonstration the KIF5A expression is reduced in brains of patients with multiple sclerosis [41,42], it is intriguing to speculate that the findings presented here have relevance to neurodegenerative diseases. Furthermore, the existence of four FDA-approved HDAC inhibitors suggests an avenue for pharmacological manipulation of the HDAC/JIP1/KIF5A axis to treat cardiac and non-cardiac diseases in humans.

5. Conclusions

HDACs are promising therapeutic targets for the treatment of pathological cardiac hypertrophy and fibrosis. Increased understanding of the molecular consequences of HDAC inhibition in cardiac cells will facilitate clinical translation of HDAC inhibitors for the treatment of heart failure. The findings presented here highlight a role for HDACs in controlling expression of a MAP kinase scaffolding protein, JIP1, which feeds forward to stimulate expression of a kinesin motor protein that regulates microtubule trafficking. There is a paucity of information about JIP1 function in cardiomyocytes, and it is derived from two papers that were published near the beginning of the 21st century. Based on the data provided here, additional evaluation of the interplay between JIP1 and HDACs in the heart is warranted.

Acknowledgments

We thank Keith Koch (UCD) for advice regarding the microtubule binding assay, Kunhua Song and Congwu Chi (UCD) for assistance with LC3 measurements, and Lynn Heasley (UCD) for critical input. T.A.M. was supported by the National Institutes of Health (HL116848, HL127240 and AG043822) and the American Heart Association (16SFRN31400013). W.W.B. was funded by the University of Colorado Denver Pharmacology Program T32 Training Grant (GM007635). M.S.S. was funded by a T32 training grant and an F32 fellowship from the National Institutes of Health (5T32HL007822 and F32HL126354). Y.H.L. was supported by an American Heart Association postdoctoral fellowship (16POST30960017).

References

1. Choudhary C, Kumar C, Gnad F, Nielsen ML, Rehman M, Walther TC, et al. Lysine acetylation targets protein complexes and co-regulates major cellular functions. Science. 2009; 325:834–840. [PubMed: 19608861]
2. Choudhary C, Weinert BT, Nishida Y, Verdin E, Mann M. The growing landscape of lysine acetylation links metabolism and cell signalling. Nat Rev Mol Cell Biol. 2014; 15:536–550. [PubMed: 25053359]
3. Lundby A, Lage K, Weinert BT, Bekker-Jensen DB, Secher A, Skovgaard T, et al. Proteomic analysis of lysine acetylation sites in rat tissues reveals organ specificity and subcellular patterns. Cell Rep. 2012; 2:419–431. [PubMed: 22902405]
4. Gregoretti IV, Lee YM, Goodson HV. Molecular evolution of the histone deacetylase family: functional implications of phylogenetic analysis. J. Mol. Biol. 2004; 338:17–31. [PubMed: 15050820]

5. McKinsey TA, Kass DA. Small-molecule therapies for cardiac hypertrophy: moving beneath the cell surface. Nat. Rev. Drug Discov. 2007; 6:617–635. [PubMed: 17643091]
6. Mozaffarian D, Benjamin EJ, Go AS, Arnett DK, Blaha MJ, Cushman M, et al. Executive summary: heart disease and stroke statistics–2016 update: a report from the American Heart Association. Circulation. 2016; 133:447–454. [PubMed: 26811276]
7. McKinsey TA. Therapeutic potential for HDAC inhibitors in the heart. Annu. Rev. Pharmacol. Toxicol. 2012; 52:303–319. [PubMed: 21942627]
8. Cao DJ, Wang ZV, Battiprolu PK, Jiang N, Morales CR, Kong Y, et al. Histone deacetylase (HDAC) inhibitors attenuate cardiac hypertrophy by suppressing autophagy. Proc. Natl. Acad. Sci. U. S. A. 2011; 108:4123–4128. [PubMed: 21367693]
9. Bradner JE, West N, Grachan ML, Greenberg EF, Haggarty SJ, Warnow T, et al. Chemical phylogenetics of histone deacetylases. Nat. Chem. Biol. 2010; 6:238–243. [PubMed: 20139990]
10. McKinsey TA, Olson EN. Dual roles of histone deacetylases in the control of cardiac growth. Novartis Found. Symp. 2004; 259:132–141. [PubMed: 15171251]
11. Kee HJ, Eom GH, Joung H, Shin S, Kim JR, Cho YK, et al. Activation of histone deacetylase 2 by inducible heat shock protein 70 in cardiac hypertrophy. Circ. Res. 2008; 103:1259–1269. [PubMed: 18849323]
12. Gallo P, Latronico MV, Gallo P, Grimaldi S, Borgia F, Todaro M, et al. Inhibition of class I histone deacetylase with an apicidin derivative prevents cardiac hypertrophy and failure. Cardiovasc. Res. 2008; 80:416–424. [PubMed: 18697792]
13. Morales CR, Li DL, Pedrozo Z, May HI, Jiang N, Kyrychenko V, et al. Inhibition of class I histone deacetylases blunts cardiac hypertrophy through TSC2-dependent mTOR repression. Sci. Signal. 2016; 9:ra34. [PubMed: 27048565]
14. Williams SM, Golden-Mason L, Ferguson BS, Schuetze KB, Cavasin MA, Demos-Davies K, et al. Class I HDACs regulate angiotensin II-dependent cardiac fibrosis via fibroblasts and circulating fibrocytes. J. Mol. Cell. Cardiol. 2014; 67:112–125. [PubMed: 24374140]
15. Nural-Guvener HF, Zakharova L, Nimlos J, Popovic S, Mastroeni D, Gaballa MA. HDAC class I inhibitor, Mocetinostat, reverses cardiac fibrosis in heart failure and diminishes CD90 + cardiac myofibroblast activation. Fibrogenesis Tissue Repair. 2014; 7:10. [PubMed: 25024745]
16. Cunliffe VT. Eloquent silence: developmental functions of Class I histone deacetylases. Curr. Opin. Genet. Dev. 2008; 18:404–410. [PubMed: 18929655]
17. Kelly RD, Cowley SM. The physiological roles of histone deacetylase (HDAC) 1 and 2: complex co-stars with multiple leading parts. Biochem. Soc. Trans. 2013; 41:741–749. [PubMed: 23697933]
18. Kee HJ, Kook H. Kruppel-like factor 4 mediates histone deacetylase inhibitor-induced prevention of cardiac hypertrophy. J. Mol. Cell. Cardiol. 2009; 47:770–780. [PubMed: 19729022]
19. Stratton MS, Lin CY, Anand P, Tatman PD, Ferguson BS, Wickers ST, et al. Signal-dependent recruitment of BRD4 to cardiomyocyte super-enhancers is suppressed by a microRNA. Cell Rep. 2016; 16:1366–1378. [PubMed: 27425608]
20. Schuetze KB, Stratton MS, Blakeslee WW, Wempe MF, Wagner FF, Holson EB, et al. Overlapping and divergent actions of structurally distinct histone deacetylase inhibitors in cardiac fibroblasts. J. Pharmacol. Exp. Ther. 2017; 361:140–150. [PubMed: 28174211]
21. Renaud L, Harris LG, Mani SK, Kasiganesan H, Chou JC, Baicu CF, et al. HDACs regulate miR-133a expression in pressure overload-induced cardiac fibrosis. Circ Heart Fail. 2015; 8:1094–1104. [PubMed: 26371176]
22. Ferguson BS, Harrison BC, Jeong MY, Reid BG, Wempe MF, Wagner FF, et al. Signal-dependent repression of DUSP5 by class I HDACs controls nuclear ERK activity and cardiomyocyte hypertrophy. Proc. Natl. Acad. Sci. U. S. A. 2013; 110:9806–9811. [PubMed: 23720316]
23. Dickens M, Rogers JS, Cavanagh J, Raitano A, Xia Z, Halpern JR, et al. A cytoplasmic inhibitor of the JNK signal transduction pathway. Science. 1997; 277:693–696. [PubMed: 9235893]
24. Trapnell C, Williams BA, Pertea G, Mortazavi A, Kwan G, van Baren MJ, et al. Transcript assembly and quantification by RNA-Seq reveals unannotated transcripts and isoform switching during cell differentiation. Nat. Biotechnol. 2010; 28(5):511. [PubMed: 20436464]

25. Ling Z, Van de Casteele M, Dong J, Heimberg H, Haefliger JA, Waeber G, et al. Variations in IB1/JIP1 expression regulate susceptibility of beta-cells to cytokine-induced apoptosis irrespective of C-Jun NH2-terminal kinase signaling. Diabetes. 2003; 52:2497–2502. [PubMed: 14514632]
26. Kim IJ, Lee KW, Park BY, Lee JK, Park J, Choi IY, et al. Molecular cloning of multiple splicing variants of JIP-1 preferentially expressed in brain. J. Neurochem. 1999; 72:1335–1343. [PubMed: 10098834]
27. Fu MM, Holzbaur EL. Integrated regulation of motor-driven organelle transport by scaffolding proteins. Trends Cell Biol. 2014; 24:564–574. [PubMed: 24953741]
28. Fu MM, Holzbaur EL. MAPK8IP1/JIP1 regulates the trafficking of autophagosomes in neurons. Autophagy. 2014; 10:2079–2081. [PubMed: 25483967]
29. Fu MM, Nirschl JJ, Holzbaur EL. LC3 binding to the scaffolding protein JIP1 regulates processive dynein-driven transport of autophagosomes. Dev. Cell. 2014; 29:577–590. [PubMed: 24914561]
30. Finn SG, Dickens M, Fuller SJ. c-Jun N-terminal kinase-interacting protein 1 inhibits gene expression in response to hypertrophic agonists in neonatal rat ventricular myocytes. Biochem. J. 2001; 358:489–495. [PubMed: 11513749]
31. He H, Li HL, Lin A, Gottlieb RA. Activation of the JNK pathway is important for cardiomyocyte death in response to simulated ischemia. Cell Death Differ. 1999; 6:987–991. [PubMed: 10556976]
32. Kolodziejczyk SM, Walsh GS, Balazsi K, Seale P, Sandoz J, Hierlihy AM, et al. Activation of JNK1 contributes to dystrophic muscle pathogenesis. Curr. Biol. 2001; 11:1278–1282. [PubMed: 11525743]
33. Fu MM, Holzbaur EL. JIP1 regulates the directionality of APP axonal transport by coordinating kinesin and dynein motors. J. Cell Biol. 2013; 202:495–508. [PubMed: 23897889]
34. Horiuchi D, Barkus RV, Pilling AD, Gassman A, Saxton WM. APLIP1, a kinesin binding JIP-1/JNK scaffold protein, influences the axonal transport of both vesicles and mitochondria in Drosophila. Curr. Biol. 2005; 15:2137–2141. [PubMed: 16332540]
35. Muresan Z, Muresan V. c-Jun NH2-terminal kinase-interacting protein-3 facilitates phosphorylation and controls localization of amyloid-beta precursor protein. J. Neurosci. 2005; 25:3741–3751. [PubMed: 15829626]
36. Xie M, Kong Y, Tan W, May H, Battiprolu PK, Pedrozo Z, et al. Histone deacetylase inhibition blunts ischemia/reperfusion injury by inducing cardiomyocyte autophagy. Circulation. 2014; 129:1139–1151. [PubMed: 24396039]
37. Abderrahmani A, Steinmann M, Plaisance V, Niederhauser G, Haefliger JA, Mooser V, et al. The transcriptional repressor REST determines the cell-specific expression of the human MAPK8IP1 gene encoding IB1 (JIP-1). Mol. Cell. Biol. 2001; 21:7256–7267. [PubMed: 11585908]
38. Huang Y, Myers SJ, Dingledine R. Transcriptional repression by REST: recruitment of Sin3A and histone deacetylase to neuronal genes. Nat. Neurosci. 1999; 2:867–872. [PubMed: 10491605]
39. Dhanasekaran DN, Kashef K, Lee CM, Xu H, Reddy EP. Scaffold proteins of MAP-kinase modules. Oncogene. 2007; 26:3185–3202. [PubMed: 17496915]
40. Fichera M, Lo GM, Falco M, Sturnio M, Amata S, Calabrese O, et al. Evidence of kinesin heavy chain (KIF5A) involvement in pure hereditary spastic paraplegia. Neurology. 2004; 63:1108–1110. [PubMed: 15452312]
41. Hares K, Kemp K, Rice C, Gray E, Scolding N, Wilkins A. Reduced axonal motor protein expression in non-lesional grey matter in multiple sclerosis. Mult. Scler. 2014; 20:812–821. [PubMed: 24144874]
42. Hares K, Redondo J, Kemp K, Rice C, Scolding N, Wilkins A. Axonal motor protein KIF5A and associated cargo deficits in multiple sclerosis lesional and normal-appearing white matter. Neuropathol. Appl. Neurobiol. 2017; 43:227–241. [PubMed: 26785938]

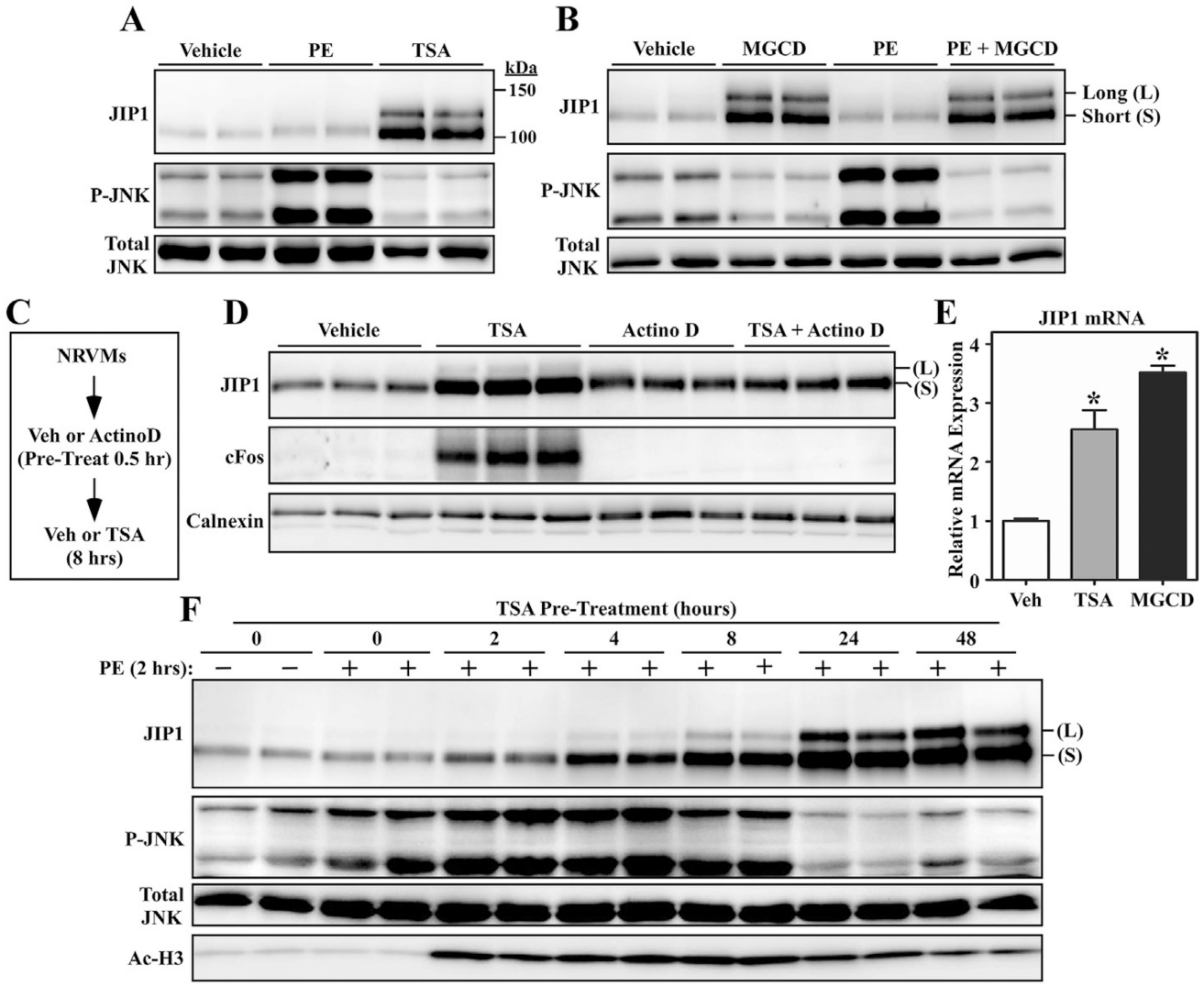

Fig. 1.

HDAC inhibition in cardiomyocytes triggers concomitant induction of JIP1 and repression of JNK phosphorylation. (A) Neonatal rat ventricular myocytes (NRVMs) were treated with vehicle control (0.1% DMSO, final concentration), phenylephrine (PE; 10 μM) or trichostatin A (TSA; 200 nM) for 48 h. Whole cell protein homogenates were immunoblotted with the indicated antibodies. TSA treatment led to increased expression of two isoforms of JIP1, with a parallel downregulation of basal JNK phosphorylation. (B) NRVMs were treated with the class I HDAC inhibitor MGCD0103 (MGCD; 1 μM) in the absence or presence of PE for 48 h. Class I HDAC inhibition stimulated expression of two isoforms of JIP1, which are referred to as JIP1(L) and JIP1(S), and reduced basal and PE-induced JNK phosphorylation. (C) Experimental design for data shown in (D). (D) NRVMs were treated with actinomycin D (Actino D; 1 μg/ml); pretreatment blocked HDAC inhibitor-mediated induction of JIP1 protein expression. The product of the immediate early gene, cFos, served as a positive control for actinomycin D action, and calnexin was a loading control. (E) TSA and MGCD treatment of NRVMs for 48 h promoted JIP1 mRNA expression, as determined by qPCR. Values represent means + SEM. $N = 4$ per condition; $*P$

< 0.05 vs. vehicle control. (F) NRVMs were pretreated with TSA for the indicated periods prior to stimulation with PE for two hours. Immunoblotting revealed that the kinetics of TSA-mediated induction of JIP1 correlate with downregulation of JNK phosphorylation. Increased acetylation of histone H3 confirmed that TSA inhibited HDAC catalytic activity in the cells.

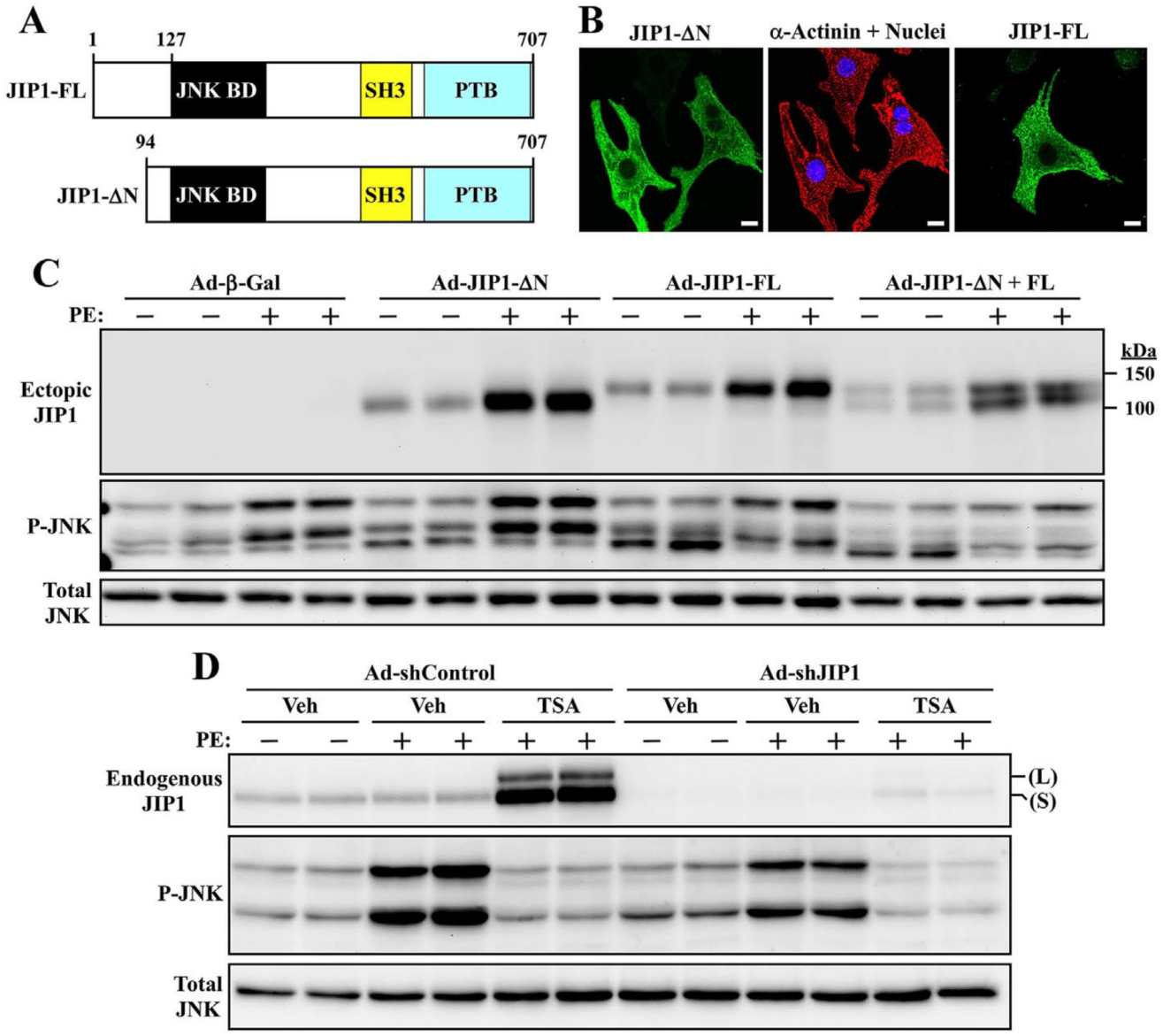

Fig. 2.

JIP1 minimally impacts JNK phosphorylation in cardiomyocytes. (A) Schematic representations of the JIP1-FL and JIP-ΔN expression constructs. JNK BD, JNK binding domain; SH3, Src Homology 3 Domain; PTB, phosphotyrosine-binding domain. (B) NRVMs were infected with adenovirus encoding Myc-tagged JIP-ΔN or FLAG-tagged JIP1-L. Indirect immunofluorescence with anti-Myc and anti-FLAG antibodies was employed to determine the subcellular distribution of ectopic JIP1 proteins (green). An anti-α-actinin antibody confirmed that the cells were cardiomyocytes (red). Scale bar = 10 μm. (C) NRVMs were infected with adenovirus encoding β-galactosidase control (β-Gal), JIP1-ΔN, JIP1-FL or both JIP1-ΔN and JIP1-FL. After overnight infection, cell were placed in serum-free medium for 24 h, and subsequently stimulated with phenylephrine (PE; 10 μM) for 2 h. Protein homogenates were prepared and immunoblotted with the indicated antibodies. The increase in ectopic JIP1 expression in PE treated cells is due to agonist-dependent induction

of the CMV promoter in the adenovirus construct. (D) NRVMs were infected with adenovirus encoding non-targeting control shRNA (Ad-shControl) or an shRNA targeting JIP1 (Ad-shJIP1). After 36 h of infection, cells were treated with vehicle or TSA (200 nM) for 24 h, and subsequently stimulated with PE (10 μM) for two hours. Protein homogenates were prepared and immunoblotted with the indicated antibodies. (For interpretation of the references to colour in this figure legend, the reader is referred to the web version of this article.)

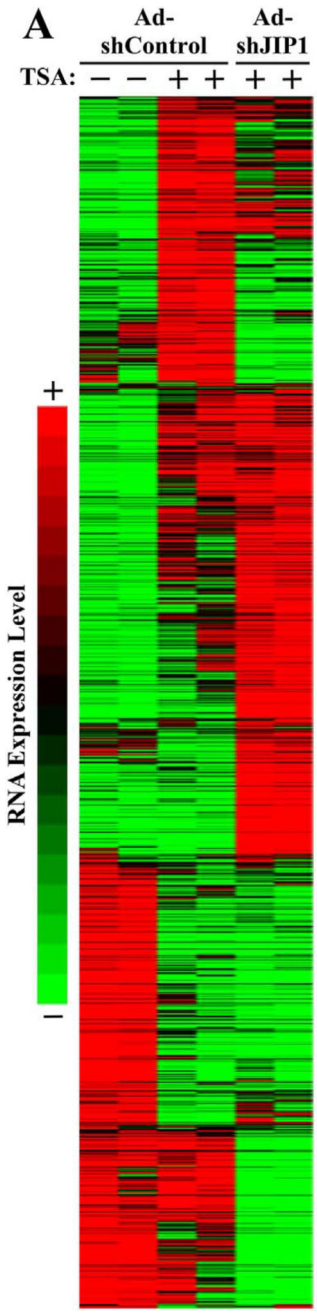

B

JIP1-Dependent Gene Expression in TSA-Treated NRVMs	
Gene Ontogeny Enrichment Set	***P*-Value**
Cytoplasmic Membrane Bound Vesicle	0.004539
Synaptic Vesicle	0.010256
Nervous System Development	0.013049
Clathrin Coated Vesicle	0.013051
Secretion	0.014523
Regulation of Transport	0.021703
Synaptic Transmission	0.021879
Regulated Secretory Pathway	0.023669
Microtubule Based Movement	0.030242
Cytoskeleton Dependent Intracellular Transport	0.042857

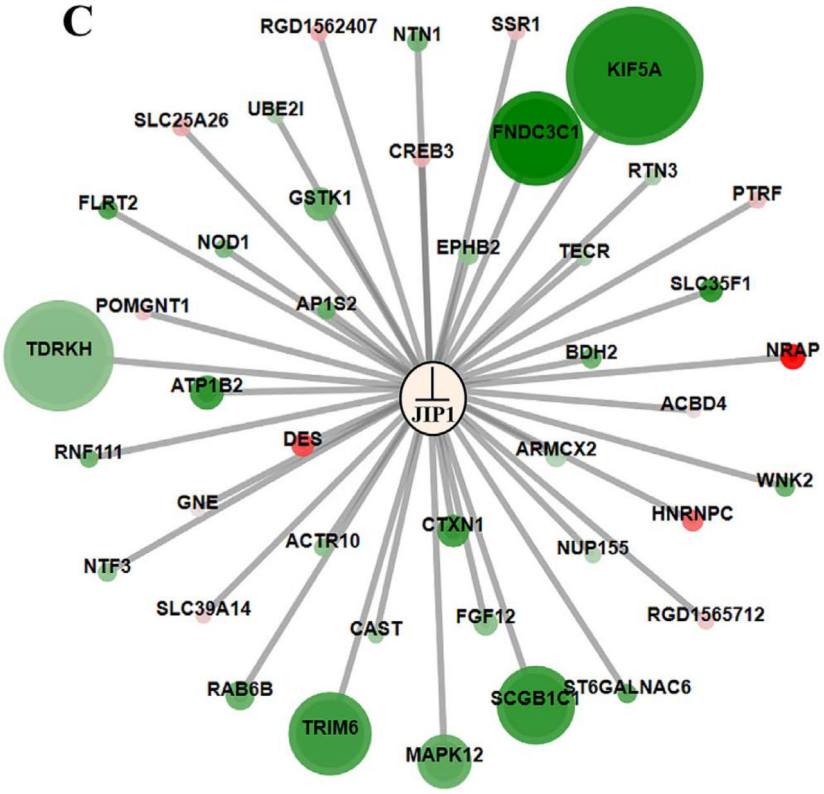

Fig. 3.

JIP1-dependent regulation of cardiac gene expression following HDAC inhibitor treatment. (A) NRVMs were infected with adenovirus encoding non-targeting control shRNA (Ad-shControl) or an shRNA targeting JIP1 (AdshJIP1) for 24 h. The cells were then treated with vehicle control (−) or TSA (200 nM) for 48 h prior to preparing total RNA for RNA-seq analysis of transcriptome-wide gene expression patterns. (B) Inspection of significantly enriched gene pathways using GSEA highlighted a pattern of JIP1- dependent gene expression associated with cytoskeleton dynamics and vesicle trafficking. (C) Network interaction analysis indicates the strength (magnitude of change indicated by the size of the

node) and direction of the expression changes (indicated by the colour of the node) between JIP1 knockdown NRVMs treated with TSA and control cells treated with TSA. KIF5A mRNA expression was most strongly associated with JIP1 expression (green = −decreased expression; red = increased expression). (For interpretation of the references to colour in this figure legend, the reader is referred to the web version of this article.)

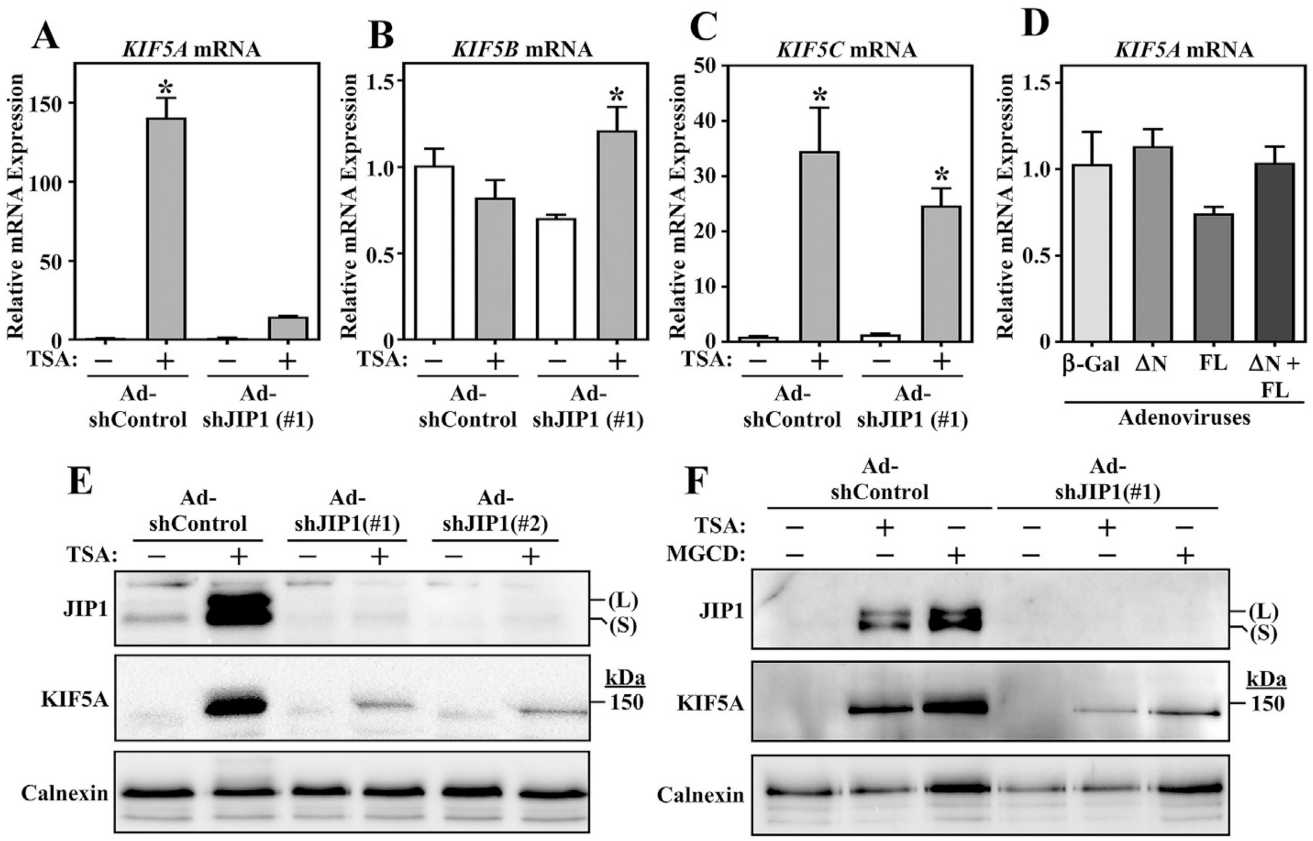

Fig. 4.

HDAC inhibitor-mediated induction of KIF5A expression requires JIP1. (A–C) NRVMs were infected with adenovirus encoding non-targeting control shRNA (Ad-shControl) or an shRNA targeting JIP1 (Ad-shJIP1#1). The cells were then treated with vehicle control (−) or TSA (200 nM) for 48 h prior to preparing total RNA for qPCR analysis of KIF5A, KIF5B and KIF5C mRNA expression. $N = 3$ per condition. Data are presented as mean + SEM; $*P < 0.05$ vs. vehicle treated cells with the same virus treatment, determined by ANOVA using Tukey's *post-hoc* test. (D) NRVMs were infected with adenovirus encoding β-galactosidase control (β-Gal), JIP1-ΔN, JIP1-FL or both JIP1-ΔN and JIP1-FL. After overnight infection cells were placed in serum-free medium for 48 h prior to harvesting RNA for KIF5A qPCR analysis. (E) NRVMs were infected with Ad-shControl, Ad-shJIP1(#1) or an adenovirus targeting independent sequences in the JIP1 transcript (AdshJIP1(#2)) for 24 h. Cells were then treated with vehicle control or TSA for 48 h prior to preparing protein homogenates for immunoblotting with antibodies specific for JIP1 and KIF5A. Calnexin served as a loading control. (F) NRVMs were infected and treated with vehicle or TSA, as in (E). In addition parallel plates of cells were treated with the class I HDAC inhibitor MGCD0103 (1 μM).

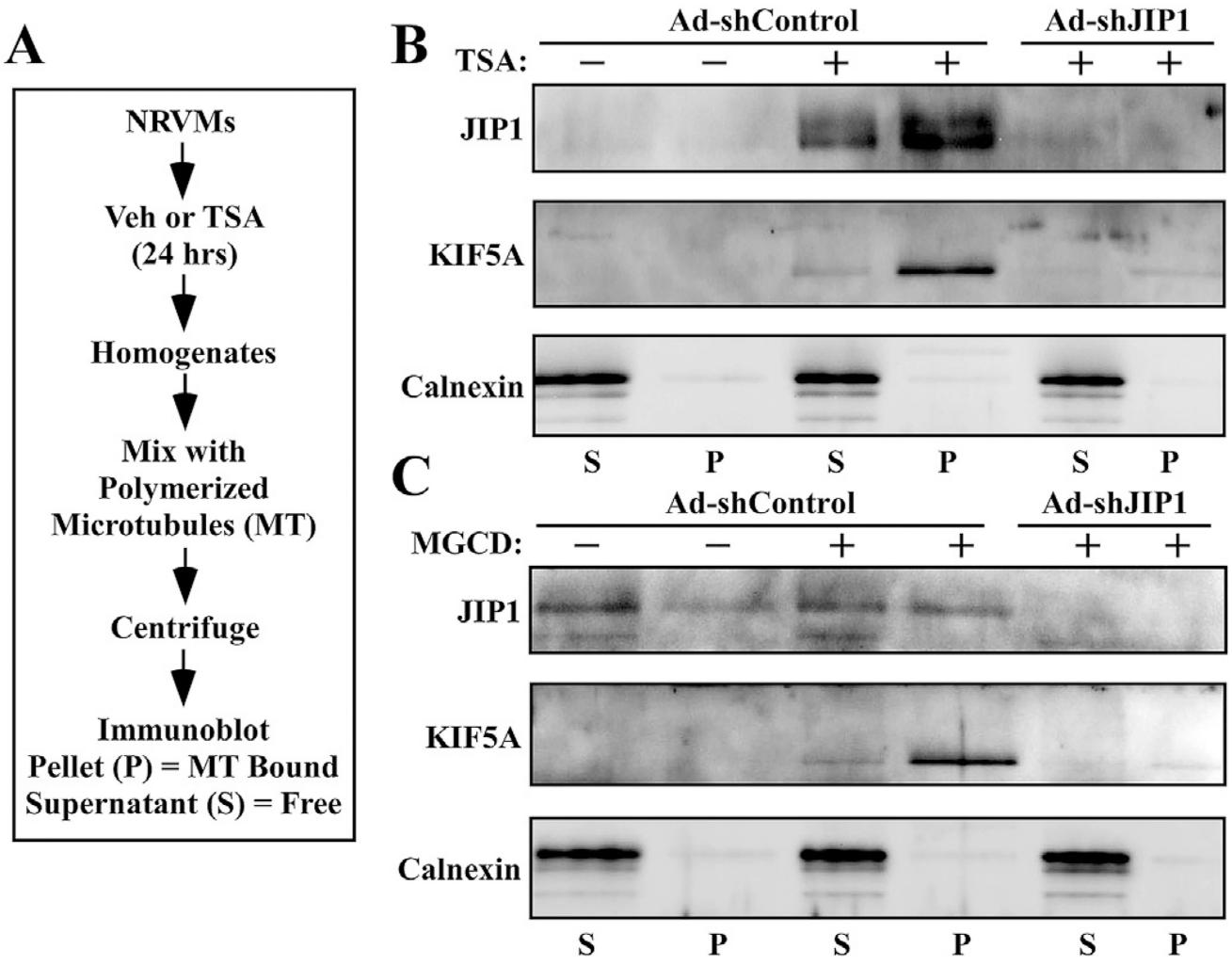

Fig. 5.

HDAC inhibition increases the ability of JIP1 and KIF5A to associate with microtubules. (A) Experimental design. (B and C) NRVMs were infected with Ad-shControl or Ad-shJIP1 for 24 h prior to treatment with TSA (B; 200 nM), MGCD0103 (C; 1 μM) or vehicle control for 48 additional hours. Protein homogenates were mixed with polymerized microtubules and separated into bound (pellet, P) and unbound (soluble, S) fractions prior to immunoblotting with the indicated antibodies.

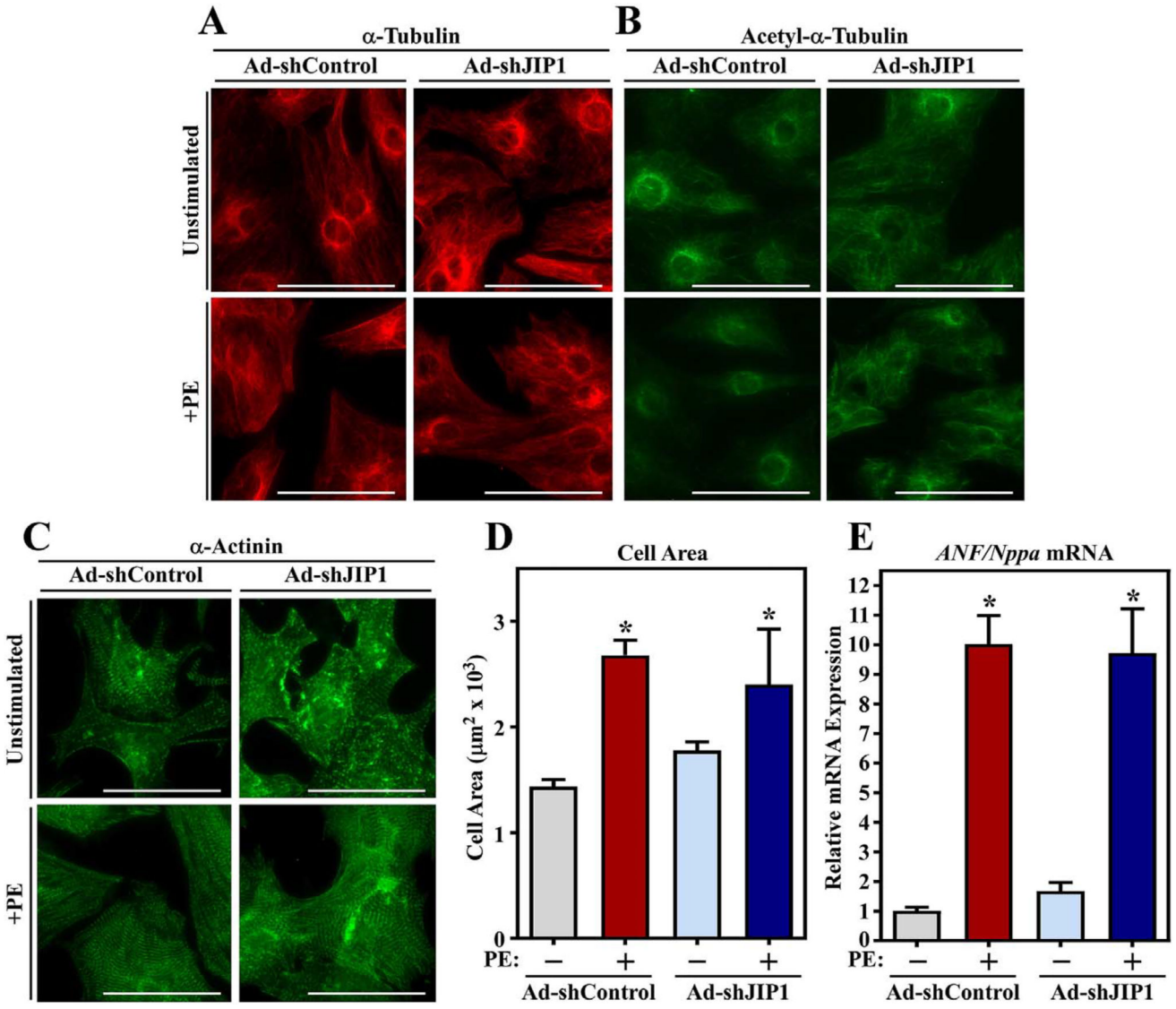

Fig. 6.

Impact of JIP1 knockdown on cardiomyocyte microtubules and agonist-dependent hypertrophy. (A–C) NRVMs were infected with adenovirus encoding non-targeting control shRNA (Ad-shControl) or an shRNA targeting JIP1 (Ad-shJIP1). After overnight infection, cells were placed in serum free medium for 8 h prior stimulation with PE (10 μM) for 48 h. Cells were fixed and analyzed by indirect immunofluorescence with the indicated antibodies. Scale bar =50 μm. (D) The area of cells in (C) was quantified. Values represent means + SEM. $N = 20$ per cells condition; $^*P < 0.05$ vs. Ad-shControl + vehicle control. (E) RNA was prepared from parallel plates of NRVMs and *Nppa* mRNA expression was assessed by quantitative PCR. Values represent means + SEM. $N = 4$ per condition; $^*P < 0.05$ vs. Ad-shControl + vehicle control.

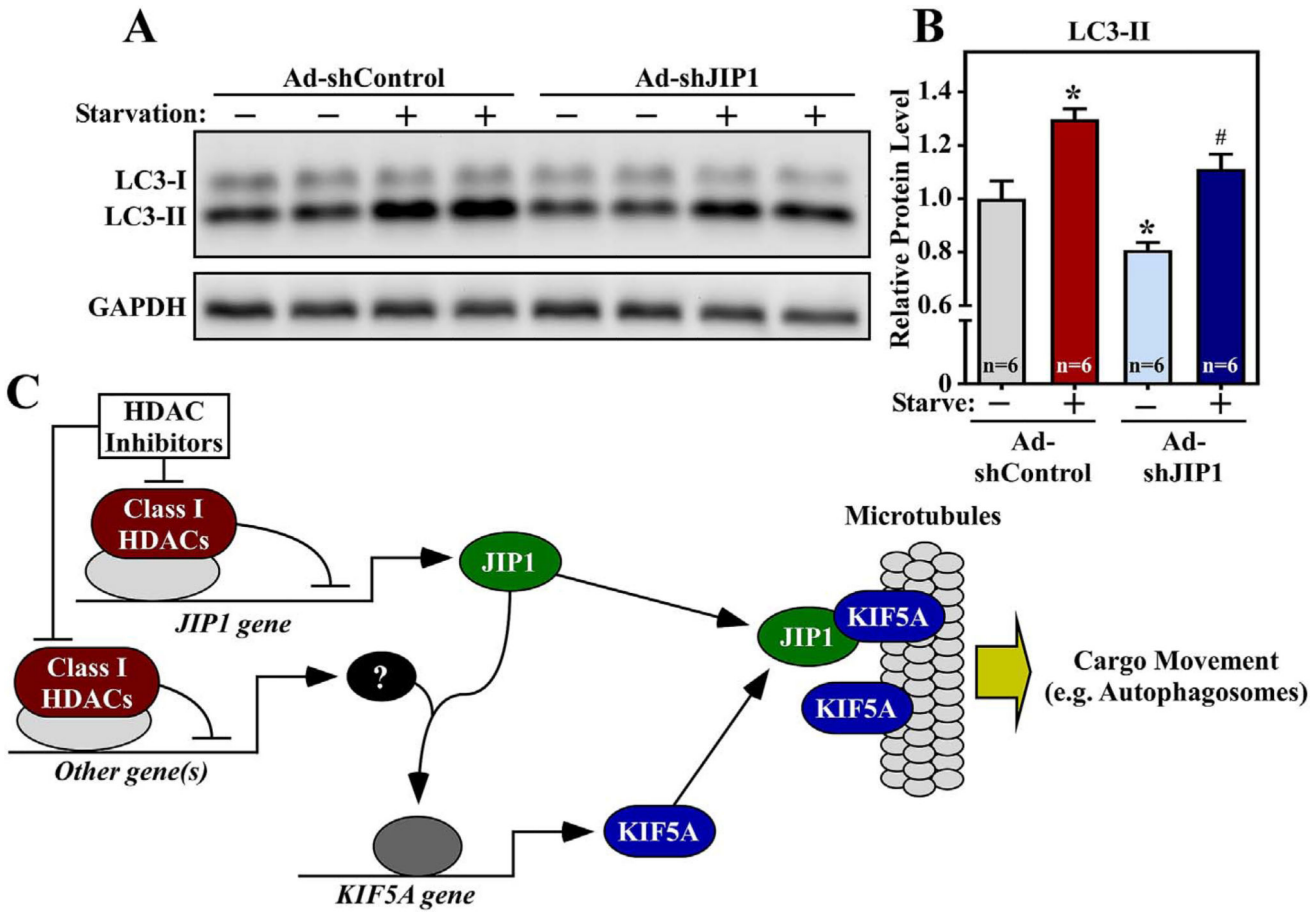

Fig. 7.

JIP1 knockdown alters autophagy in cardiomyocytes. (A) NRVMs were infected with adenovirus encoding non-targeting control shRNA (Ad-shControl) or an shRNA targeting JIP1 (Ad-shJIP1). Some cells were subjected to starvation, as described in the Materials and methods section. Whole cell homogenates were subjected to immunoblotting with the indicated antibodies. A representative immunoblot is shown. (B) The impact of JIP1 knockdown on LC3-II levels was quantified by densitometry. *$P < 0.05$ vs. Ad-shControl (minus starvation); #P < 0.05 vs. Ad-shControl (plus starvation). (C) A model depicting the mechanisms by which class I HDACs and JIP1 promote binding of the KIF5A motor protein to microtubules and alter transport of cargo along microtubules. JIP1 is necessary for HDAC inhibitor-mediated induction of KIF5A, but is not sufficient to induce KIF5A on its own. This indicates that another HDAC inhibitor-inducible factor(s), depicted as a question mark, contributes to JIP1-dependent KIF5A expression.

Table 1

Application	Target	Forward Primer	Reverse Primer
qPCR	JIP1	5′-CCA CGC TCA ACC TTT TCC C-3′	5′-AGA TAT GTT CAT GTG GAG GCG-3′
	KIF5A	5′-AGG TGC TGA ATG GAC TGA TG-3′	5′-ACC TCT GAC TTG ATC TTG CTG-3′
	KIF5B	5′-ACG AGT CTG AAG TGA ACC GC-3′	5′-GCT TGG ACG CAA TCA TCA CC-3′
	KIF5C	5′-CCA GGA TCG CAC ACG ATA TT-3′	5′-ACG TCA AGC AAG TCC CTT ATT-3′
	Nppa/ANF ΔN	5′-GCC GGT AGA AGA TGA GGT CAT G-3′	5′-GCT TCC TCA GTC TGC TCA CTC A-3′
Cloning JIP1		5′- CC ATCGAT GAC CTG ATC GAC GCG GCA GGT GAC ACT-3′	5′- CGG AAT TCC TAC TCC AAG TAG ATA TCT TCT GTA GG-3′
	Full-Length	5′- GGG GTA CCC CAC CAT GGA TTA TAA GGA TGA CGA C-3′	5′- CGG AAT TCC TAC TCC AAG TAG ATA TCT TCT GTA GG-3′
shRNA oligos annealed and ligated into pENTR/U6	shControl	5′-ACC GCG CGA TAG CGC TAA TAA TTT CTC GAG AAA TTA TTA GCG CTA TCG CGC-3′	5′-AAA AGC GCG ATA GCG CTA ATA ATT TCT CGA GAA ATT ATT AGC GCT ATC GCG C-3′
	shJIP1 #1	5′-CAC CCA CGC TGA ATA ATA ACT CTT TCT CGA GAA AGA GTT ATT ATT CAG CGT G-3′	5′-AAA ACA CGC TGA ATA ATA ACT CTT TCT CGA GAA AGA GTT ATT ATT CAG CGT G-3′
	shJIP1 #2	5′-CAC CGT GTC TGA AGA TTC CAC CAA ACT CGA GTT TGG TGG AAT CTT CAG ACA C-3′	5′-AAA AGT GTC TGA AGA TTC CAC CAA ACT CGA GTT TGG TGG AAT CTT CAG ACA C-3′